

The High-Energy Particle Detector (HEPD-01) as a space weather monitoring instrument on board the CSES-01 satellite

Francesco Palma,^{a,*} Matteo Martucci,^{a,b} Alexandra Parmentier,^a Mirko Piersanti^c and Alessandro Sotgiu^{a,b} on behalf of the LIMADOU-HEPD Collaboration
(a complete list of authors can be found at the end of the proceedings)

^aINFN-Sezione di Roma Tor Vergata,
V. della Ricerca Scientifica 1, I-00133 Rome, Italy

^bUniversity of Rome “Tor Vergata”,
V. della Ricerca Scientifica 1, I-00133 Rome, Italy

^cINAF-IAPS,
V. Fosso del Cavaliere 100, I-00133 Rome, Italy

*At ASI Space Science Data Center (SSDC) also,
V. del Politecnico, I-00133 Rome, Italy

E-mail: francesco.palma@roma2.infn.it

CSES-01 (China Seismo-Electromagnetic Satellite) is the first element of an extended constellation of LEO (Low Earth Orbit) satellites, dedicated to monitoring perturbations of electromagnetic fields, plasma and charged particle fluxes induced by natural sources and artificial emitters in the near-Earth space. One of the nine payloads on board CSES-01 is the Italian High-Energy Particle Detector (HEPD-01), which is equipped with a silicon tracker and a range calorimeter to detect electrons (3-100 MeV), protons (30-250 MeV), and light nuclei. Since the launch of CSES-01 in February 2018, HEPD-01 has already returned valuable information about variations in the Earth-Sun interaction during geomagnetic-storm transients. One of such events was the G3-class geomagnetic storm that impacted the Earth’s magnetosphere in late August 2018, causing a temporary rearrangement of the charged particle environment around the planet. In this work, the HEPD-01 response to this magnetospheric disturbance is presented on the base of particle rate variation measurements. The study of such events is crucial to better understand mechanisms taking place during solar events and to prevent their harmful effects on technological and anthropic systems, as well as on human health. The presented results confirm the HEPD-01 capabilities in monitoring the near-Earth environment and contributing to establish a nowcasting/forecasting network in the nearest possible future.

37th International Cosmic Ray Conference (ICRC 2021)
July 12th – 23rd, 2021
Online – Berlin, Germany

*Presenter

1. Introduction

Space weather refers to those effects such as reduced satellite operations, failures in spacecraft electronics, radio communication problems from perturbations in the Earth's ionosphere, and even downed power grids during major geomagnetic storms [1].

Magnetic storms represent major signatures of variability in the Sun-Earth interaction. Such events appear as magnetic disturbances caused by bursts of radiation and charged particles emitted from the Sun in the form of coronal mass ejections, solar flares, co-rotating interaction regions, etc. [2, 3]. These nonlinear and multiscale processes involve a vast set of plasma regions in the mutually interacting magnetosphere and ionosphere.

The terrestrial magnetosphere is under the permanent action of the solar wind. An increase in the solar wind dynamic pressure and a southward direction of the interplanetary magnetic field are considered among the fundamental factors in magnetic storm development [4, 5]. Under the solar wind driver, global changes occur in the magnetosphere following two principal dynamic triggers: magnetic reconnection at the dayside magnetopause [6] and viscous-like interactions causing magnetospheric convection [7]. One major consequence is the change in the fluxes of charged particles that constitute the magnetospheric ring current. In cascade, the magnetosphere, which is mapped to the upper ionosphere through a system of field-aligned currents, can exchange momentum, energy, and particles with the latter by means of a variety of interactions. Discerning physical phenomena that mark the solar-terrestrial environment is not the sole goal of the investigation of storm phenomena, since geomagnetic storms and substorms can severely impact infrastructures at the ground level and in space, also posing a hazard to human health [8].

On 20th August 2018, a large-scale filament gradually erupted from a quiet region of the Sun into an interplanetary coronal mass ejection (ICME) that affected the Earth's environment a few days later, starting on late 25th August 2018 [9] and giving rise to the third largest storm of Solar Cycle 24. The magnetospheric disturbance was strong enough to trigger a response in the High-Energy Particle Detector (HEPD-01) on board the China Seismo-Electromagnetic Satellite (CSES-01).

2. The High-Energy Particle Detector (HEPD-01)

The High-Energy Particle Detector is one of the nine payloads on board the China Seismo-Electromagnetic Satellite, which is currently flying in a Sun-synchronous polar orbit at a ~ 507 km altitude with a 97° inclination and a five-day revisit time.

CSES-01 [10] was designed for the observation of variations in particle fluxes, plasma parameters, and the electromagnetic field and waves, induced by both natural and anthropogenic sources in the near-Earth space. One major goal of this Chinese-Italian space mission is to investigate possible correlations between the above-mentioned perturbations and the occurrence of high-magnitude earthquakes. Other fundamental targets are the study of space weather phenomena and cosmic ray propagation.

HEPD-01 is a light and compact ($40.36 \text{ cm} \times 53.00 \text{ cm} \times 38.15 \text{ cm}$, total mass ~ 45 kg) payload designed and built by the Limadou Collaboration, the Italian branch of the CSES mission. A schematic representation of the apparatus is reported in Figure 1. The HEPD-01 is made up of a silicon tracking system; a trigger system that includes one plastic scintillator layer segmented into

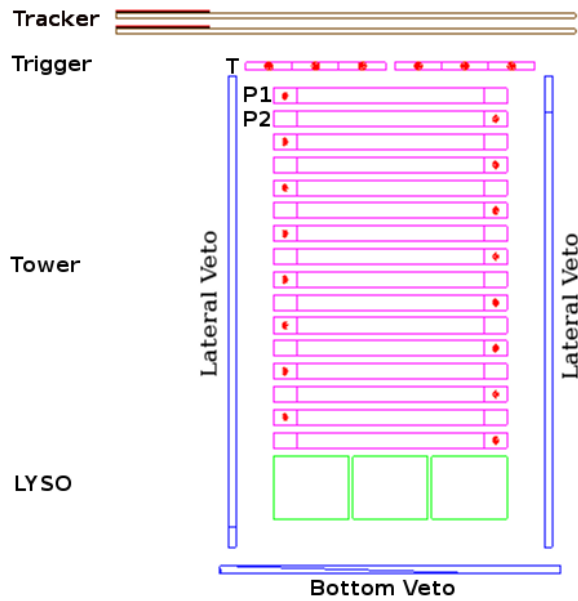


Figure 1: Schematic of the HEPD-01 detector. All mechanical structures (as well as the lateral VETO plane located in the front) have been removed from the figure for visualization purposes.

six paddles; a range calorimeter comprising a tower of 16 plastic scintillator planes, a matrix of 3×3 LYSO (lutetium–yttrium oxyorthosilicate) scintillator crystals, and an anti-coincidence (VETO) system equipped with 5 plastic scintillator planes, out of which 4 are placed at the lateral sides of the apparatus and 1 at the bottom (for further details, see [11–13]).

Thanks to this set of subdetectors, the HEPD-01 is optimized to detect electrons in the energy range between 3 and 100 MeV and protons between 30 and 250 MeV [14], as well as light nuclei. In addition, the apparatus can detect different particle populations (solar, trapped, galactic, etc.) according to the satellite position (defined by the McIlwain L-shell parameter) and detected energy. Due to adjustments in attitude and additional scheduled maneuvers, the CSES-01 payloads are usually switched off at latitudes below -65° and above $+65^\circ$. However, the HEPD-01 can benefit from its large field of view ($\pm 60^\circ$) and geometrical acceptance to collect particles at large L-shells, though for a short time per day.

In the current trigger configuration, labeled as T & P1 & P2 and set in July 2018 (late commissioning phase), the geometrical factor for electrons reaches a plateau value of $\sim 500 \text{ cm}^2 \text{ sr}$ at energies larger than $\sim 30 \text{ MeV}$. T & P1 & P2 corresponds to event acquisition and processing only when the released signals in the trigger plane (T) and the first two calorimeter planes (P1, P2) are above predefined thresholds. The transmission of a dedicated command allows setting one of the eight predefined trigger mask configurations [15], which are the result of different logic combinations of counters from the various subdetectors. Hence, the different trigger masks define the aperture and the energy acceptance of the instrument. The trigger condition, labeled as T, corresponds to an above-threshold signal only in the trigger plane, and it is associated with the lowest energy threshold. By requiring a deeper penetration of the particle inside the detector (i.e., using the trigger plane counters and a set of tower planes in “AND” configuration, such as T & P1, T & P1 & P2, and so on), the geometrical factor of the HEPD-01 decreases, and consequently, the

energy threshold for triggering increases.

3. HEPD-01 response to the August 2018 storm

Figure 2 illustrates a comparison between the HEPD-01 count rate maps before (20th-23rd August; upper panel) and after the impact of the storm (25th-27th August; lower panel). In the bottom panel, an increase in the count rate is evident at both northern and southern latitudes—especially in the southern region—as a consequence of the storm’s arrival. Both maps are related

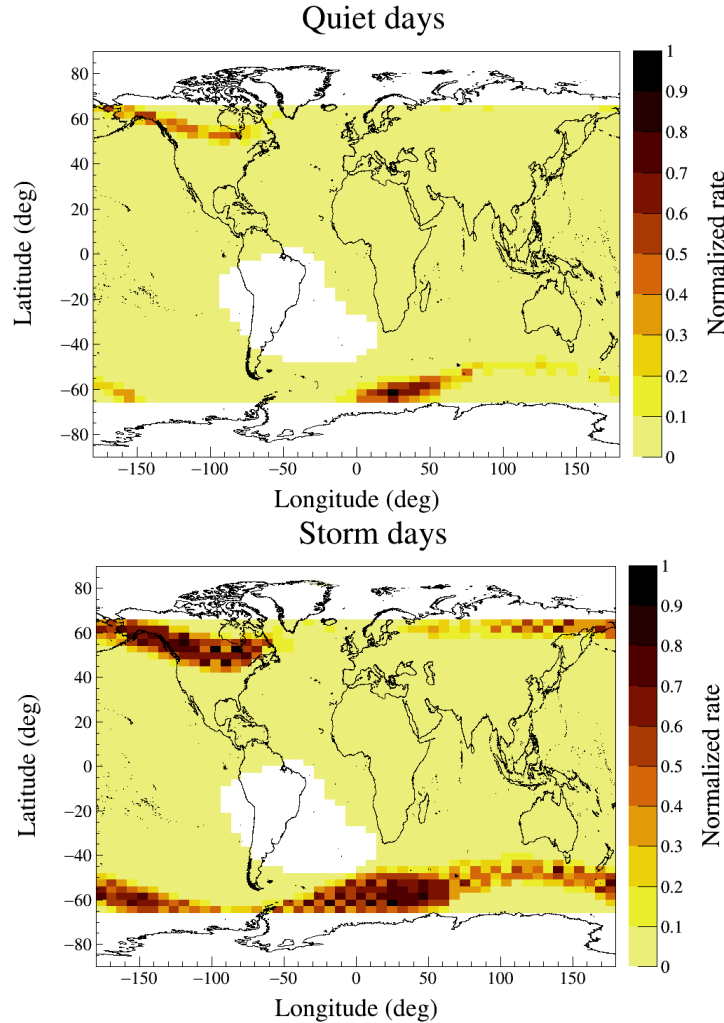


Figure 2: Comparison between an HEPD-01 trigger rate map before the occurrence of the geomagnetic storm, from 20th to 23rd August (upper panel), and after the impact of the storm, from 25th to 27th August (lower panel). The maps are related to trigger configuration T, requiring an above-threshold signal just in the trigger plane and providing the lowest energy threshold for electron detection (>3 MeV). For visualization purposes, we excluded the South Atlantic Anomaly region, characterized by extremely high particle rates.

to trigger configuration T defined in Section 2, which requires an above-threshold signal only in the trigger plane and allows detecting the lowest energetic electrons (>3 MeV). As concerns protons, their contribution to the trigger rate increase is negligible due to the absence of direct injection from

solar energetic particles (SEPs) during this specific storm event [16]. For visualization purposes, we excluded the South Atlantic Anomaly (SAA) region, which is characterized by extremely high particle rates. For this purpose, we selected magnetic field values larger than 23000 nT. For this analysis, we calculated magnetic field values by using the International Geomagnetic Reference Field (IGRF) series of mathematical models, in particular the IGRF-12 candidate [17].

The increased particle rate, during the storm time, is also visible as a function of the L-shell and time in Figure 3. The first three panels show the HEPD-01 count rates for three different trigger configurations: from top to bottom, T, T & P1, and T & P1 & P2. The increase in the number

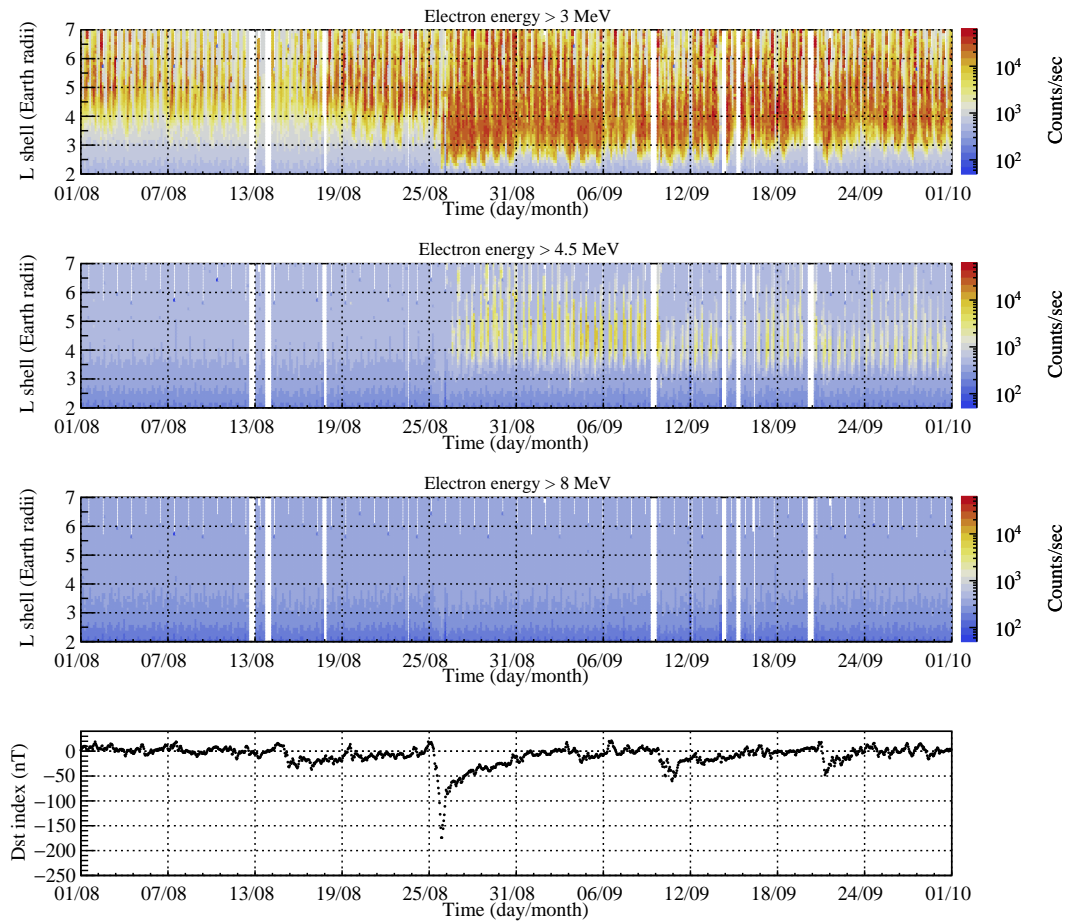


Figure 3: Top three panels: Trigger rates for three different HEPD-01 configurations over the period August-September 2018; from top to bottom, T, T & P1, and T & P1 & P2. Adding more calorimeter planes to the trigger configuration results in increasing the energy threshold for electron detection (>3 MeV for T, >4.5 MeV for T & P1, and >8 MeV for T & P1 & P2). The proton contribution to the trigger rate increase is negligible due to the absence of direct injection from SEPs. The vertical white lines are due to a lack of data. Bottom panel: Time evolution of the Dst index.

of calorimeter planes used for trigger generation resulted in a higher energy threshold for electron detection (>3 MeV, >4.5 MeV, and >8 MeV, respectively), thus reducing the particle rate. Figure 3 shows a clear enhancement during the recovery phase of the storm, which coincides with prolonged and intense substorm activity (for further discussion, see [9]). The increase can be spotted at

L-shells ≥ 3 for energies above 3 MeV (Figure 3, top panel) and, to a lesser extent, at L-shells ≥ 4 for energies above 4.5 MeV (Figure 3, second panel). Finally, for comparison, the time evolution of the Dst index is shown in the bottom panel of Figure 3. As can be inferred by a strong decrease of the Disturbance storm-time (Dst) index down to ~ -190 nT, the start of the storm's main phase was on late 25th August, exactly in coincidence with the increase of the HEPD-01 particle rates.

4. Conclusions

The study of geomagnetic storms and other space weather phenomena is crucial to better understand the mechanisms taking place during solar events and to prevent their effects on technological and anthropic systems, such as reduced satellite operations, failures in spacecraft electronics, radio communication problems, etc.

On 25th August 2018, the CSES-01/HEPD-01 particle rate meters were able to detect the effects of a G3-class, ICME-driven geomagnetic disturbance characterized by marked magnetosphere compression and plasmasphere erosion.

In our analysis, a clear enhancement of HEPD-01 count rate during the storm's recovery phase was observed. This increase was detected at L-shells ≥ 3 for electron energies above 3 MeV, and, to a lesser extent, at L-shells ≥ 4 for electron energies above 4.5 MeV. The enhancement of HEPD-01 trigger rates suggested a phenomenon of acceleration of energetic electrons, which lasted several days. Some more recent geomagnetic storm events, observed by HEPD-01, are currently under study.

Considering the sky-rocketing focus on space weather studies in this last decade, HEPD-01's results prove promising, especially in view of the already-planned constellation of CSES satellites in the next few years (CSES-02 is currently under construction). It is worth noticing that this set of satellites will take shape in a period when several other missions, which contributed to the monitoring of the near-Earth environment, will be either deactivated or well beyond the end of their scheduled lifetimes.

References

- [1] T. Cade and C. Chan-Park, *The origin of "space weather"*, *Space Weather* **13** (2015) .
- [2] J.T. Gosling, *The solar flare myth*, *J. Geophys. Res.* **98** (1993) 18937.
- [3] M. Piersanti, C. Cesaroni, L. Spogli and T. Alberti, *Does TEC react to a sudden impulse as a whole? The 2015 Saint Patrick's day storm event*, *Advances in Space Research* **60** (2017) 1807.
- [4] W.D. Gonzalez, J.A. Joselyn, Y. Kamide, H.W. Kroehl, G. Rostoker, B.T. Tsurutani et al., *What is a geomagnetic storm?*, *Journal of Geophysical Research: Space Physics* **99** (1994) 5771
[<https://agupubs.onlinelibrary.wiley.com/doi/pdf/10.1029/93JA02867>].
- [5] U. Villante and M. Piersanti, *Analysis of geomagnetic sudden impulses at low latitudes a06209*, *Journal of Geophysical Research* **114** (2009) .

- [6] J.W. Dungey, *Interplanetary magnetic field and the auroral zones*, *Phys. Rev. Lett.* **6** (1961) 47.
- [7] W. Axford and C. Hines, *A unifying theory of high latitude geophysical phenomena and magnetic storms*, *Canadian Journal of Physics* **39** (2011) 1433.
- [8] M. Hapgood, *The great storm of may 1921: An exemplar of a dangerous space weather event*, *Space Weather* **17** (2019) 950
[<https://agupubs.onlinelibrary.wiley.com/doi/pdf/10.1029/2019SW002195>].
- [9] F. Palma, A. Sotgiu, A. Parmentier, M. Martucci, M. Piersanti, S. Bartocci et al., *The august 2018 geomagnetic storm observed by the high-energy particle detector on board the cses-01 satellite.*, *Appl. Sci.* **11** (2021) 5680.
- [10] X. Shen and et al., *The state-of-the-art of the China Seismo-Electromagnetic Satellite mission*, *Science China Technological Sciences* **61** (2018) 634.
- [11] A. Ambrosi and et al., *The HEPD particle detector of the CSES satellite mission for investigating seismo-associated perturbations of the Van Allen belts*, *Science China Technological Sciences* **61** (2018) 643.
- [12] P. Picozza, R. Battiston, G. Ambrosi, S. Bartocci, L. Basara, W.J. Burger et al., *Scientific Goals and In-orbit Performance of the High-energy Particle Detector on Board the CSES*, *Astrophys. J. Suppl.* **243** (2019) 16.
- [13] G. Ambrosi, S. Bartocci, L. Basara, R. Battiston, W. Burger, D. Campana et al., *Beam test calibrations of the hepd detector on board the china seismo-electromagnetic satellite*, *Nuclear Instruments and Methods in Physics Research Section A: Accelerators, Spectrometers, Detectors and Associated Equipment* **974** (2020) 164170.
- [14] S. Bartocci, R. Battiston, W.J. Burger, D. Campana, L. Carfora, G. Castellini et al., *Galactic cosmic-ray hydrogen spectra in the 40–250 MeV range measured by the high-energy particle detector (HEPD) on board the CSES-01 satellite between 2018 and 2020*, *The Astrophysical Journal* **901** (2020) 8.
- [15] A. Sotgiu, C. De Donato, C. Fornaro, S. Tassa, M. Scannavini, D. Iannaccio et al., *Control and data acquisition software of the high-energy particle detector on board the china seismo-electromagnetic satellite space mission*, *Software: Practice and Experience* **51** (2021) 1459 [<https://onlinelibrary.wiley.com/doi/pdf/10.1002/spe.2947>].
- [16] A. Abunin, M. Abunina, A. Belov and I. Chertok, *Peculiar solar sources and geospace disturbances on 20–26 august 2018*, *Solar Physics* **295** (2020) .
- [17] E. Thébault, C.C. Finlay, C.D. Beggan, P. Alken, J. Aubert, O. Barrois et al., *International Geomagnetic Reference Field: the 12th generation*, *Earth, Planets, and Space* **67** (2015) 79.

Full Authors List: LIMADOU-HEPD Collaboration

S. Bartocci¹, R. Battiston^{2,3}, F. Benotto⁴, S. Beolé^{4,5}, W.J. Burger^{3,6}, D. Campana⁷, G. Castellini⁸, P. Cipollone¹, S. Coli⁴, L. Conti^{1,9}, A. Contin^{10,11}, M. Cristoforetti¹², L. De Cilladi^{4,5}, C. De Donato¹, C. De Santis¹, F.M. Follega^{2,3}, G. Gebbia^{2,3}, R. Iuppa^{2,3}, M. Lolli¹¹, N. Marcelli^{1,13}, M. Martucci^{1,13}, G. Masciantonio¹, M. Mergé^{1,†}, M. Mese^{7,14}, C. Neubuser³, F. Nozzoli³, A. Oliva¹¹, G. Osteria⁷, L. Pacini¹⁵, F. Palma^{1,†}, F. Palmonari^{10,11}, A. Parmentier¹, F. Perfetto⁷, P. Picozza^{1,13}, M. Piersanti¹⁶, M. Pozzato¹¹, E. Ricci^{2,3}, M. Ricci¹⁷, S.B. Ricciarini⁸, Z. Sahnoun¹¹, V. Scotti^{7,14}, A. Sotgiu^{1,13}, R. Sparvoli^{1,13}, V. Vitale¹, S. Zoffoli¹⁸ and P. Zuccon^{2,3}

¹ INFN-Sezione di Roma “Tor Vergata”, V. della Ricerca Scientifica 1, I-00133 Rome, Italy;

² University of Trento, V. Sommarive 14, I-38123 Povo (Trento), Italy;

³ INFN-TIFPA, V. Sommarive 14, I-38123 Povo (Trento), Italy;

⁴ INFN-Sezione di Torino, Via P. Giuria 1, I-10125 Torino, Italy;

⁵ University of Torino, Via P. Giuria 1, I-10125 Torino, Italy;

⁶ Centro Fermi, V. Panisperna 89a, I-00184 Rome, Italy;

⁷ INFN-Sezione di Napoli, V. Cintia, I-80126 Naples, Italy;

⁸ IFAC-CNR, V. Madonna del Piano 10, I-50019 Sesto Fiorentino (Florence), Italy;

⁹ Uninettuno University, C.so V. Emanuele II 39, I-00186 Rome, Italy;

¹⁰ University of Bologna, V.le C. Berti Pichat 6/2, I-40127 Bologna, Italy;

¹¹ INFN-Sezione di Bologna, V.le C. Berti Pichat 6/2, I-40127 Bologna, Italy;

¹² Fondazione Bruno Kessler, V. Sommarive 18, I-38123 Povo (Trento), Italy;

¹³ University of Rome “Tor Vergata”, V. della Ricerca Scientifica 1, I-00133 Rome, Italy;

¹⁴ University of Naples “Federico II”, V. Cintia 21, I-80126 Naples, Italy;

¹⁵ INFN-Sezione di Firenze, V. Sansone 1, I-50019 Sesto Fiorentino (Florence), Italy;

¹⁶ INAF-IAPS, V. Fosso del Cavaliere 100, I-00133 Rome, Italy;

¹⁷ INFN-LNF, V. E. Fermi 54, I-00044 Frascati (Rome), Italy;

¹⁸ Italian Space Agency, V. del Politecnico, I-00133 Rome, Italy;

† At ASI Space Science Data Center (SSDC) also, V. del Politecnico, I-00133 Rome, Italy.